Investigating Attenuation and Reflection of Short-Period Ocean Waves Propagating into Arctic Pack Ice

ABS098

[1,2]Matthew G. Asplin, [1]John Marko,[1]David B. Fissel and [1]Keath Borg

[1]ASL Environmental Sciences Inc., #1-6703 Rajpur Place, Victoria, British Columbia, Canada

Now at: [2]Department of Geography, University of Victoria, Victoria, British Columbia, Canada

1. Introduction & Objectives

Dramatic reductions in sea ice extent (Parkinson, 2014), thickness and volume (Laxon et al., 2013), and increasing melt season length (Stroeve et al., 2014) have been observed in the northern hemisphere. Large expanses of open water (Walsh, 2013) and commensurate increases in fetch introduce the potential for increasing regional wave energy (Thomson & Rogers, 2014) which directly impacts the remaining sea ice cover. Wave propagation penetration of sea ice increases with wave period and wavelength (Squire et al., 2009), inducing flexural fracture and ice cover break-up (Wadhams et al., 1988; Asplin et al., 2012; Collins et al., 2015). These changes rapidly increase the size of marginal ice zone (MIZ) (Collins et al., 2015), with smaller, mobile ice floes that are more susceptible to lateral melting and dynamic forcing (*e.g.* Asplin et al., 2014). Waves-in-ice (WII) events are, therefore, of great interest within the sea ice modeling community.

This poster presents an analysis of a waves-in-ice event 23 – 24 May 2011 identified within data collected during an extensive three-year program of oceanographic and ice measurements as part of the 2009 - 2011 ArcticNet-Industrial Partnership Program in support of oil and gas exploration by Imperial Oil Ltd. (IOL) and BP Ltd.

2. Data and Methods

An extensive program of oceanographic and ice measurements was carried out in the deepwater Pokak and Ajurak Licence areas. More than 50 underwater, internally-recording instruments at eight sites in water depths ranging from 73 – 1003 m for periods of 356 – 380 days were employed (Figure 1). At each measurement site, the upper instrument on the mooring was an Ice Profiling Sonar (IPS-5) instrument, operated to provide ice draft measurements at one- or two-second intervals, and non-directional wave measurements at 2 Hz sampling rates in open water. Ice velocity measurements, at 15 to 60 minutes sampling intervals, were obtained from Acoustic Doppler Current Profilers (ADCP). Wave autospectra were computed using the Fast Fourier Transform (FFT) technique. Non-directional wave parameters were then computed from the autospectra: significant wave height (H_S), calculated as four times the square root of the area under the autospectral curve; peak period (T_P), calculated as the corresponding period at which the autospectra reaches its maximum, and maximum wave height (H_{MAX}).

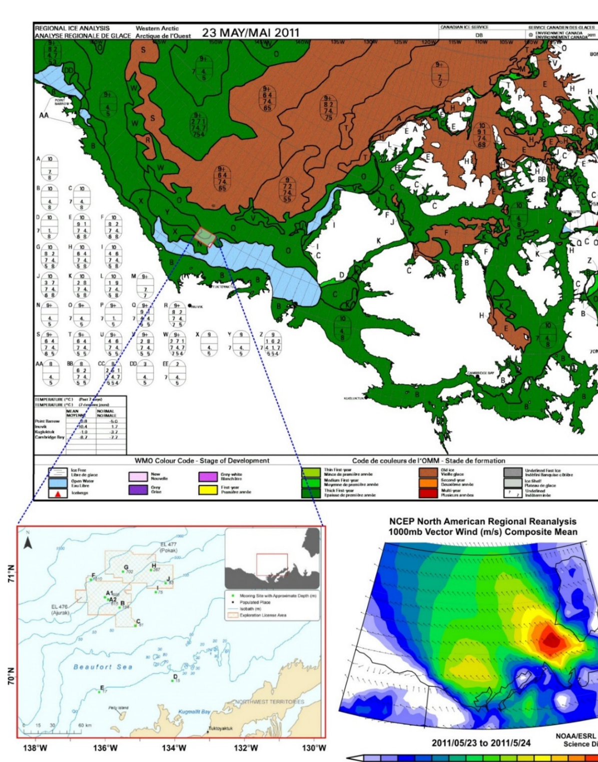

Figure 1. Top) Canadian Ice Service ice chart for 23 May 2011 with a prominent open water feature (fetch) present in the southern Beaufort Sea with significant wave height (H_S), maximum wave height (H_{MAX}), and peak period (T_P) for Site J. Bottom left) Map of Mooring Sites used in regression analysis with data covering the period 01 January 2010 – 31 May 2010 and January 2011 – 31 May 2011. Bottom Right) mean vector winds (m/s) for 23 – 24 May 2011. (Right) Typical subsurface mooring diagram showing various instruments and their position along the mooring line at a medium depth site (Site H).

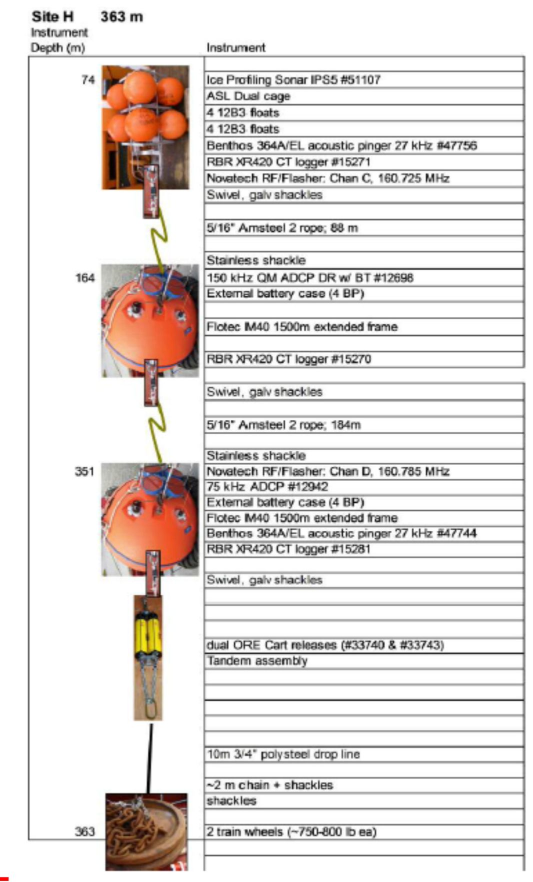

Analysis of wave propagation in ice followed the rule of thumb of Meylan et al., (2014) that ice floes typically respond to waves with lengths less than four times their diameter. Given our observed wave period of ~5 s and a calculated wavelength of l = 37.5 m ice floes with linear dimensions that are less than or equal to 10 m were utilized, to estimate wave energy attenuation coefficients a for site H and I from equation 1:

$$H(D)\,/\,H(D=0) = e^{-\alpha D}$$

where H(D) is the wave height (m) and H(D=0) is the wave height as estimated at the ice edge. Reflection coefficients were estimated by calculating the attenuation coefficient α corresponding to amplitude in the outermost ice floe and H_S as estimated in the adjacent open water region. Attenuation is assessed relative to the outermost ice floe at all points along the sampled transect where valid wave height estimates were feasible. Site J is used as an 'open water' reference for wave characteristics.

3. 23 – 24 May 2011 Waves-in-Ice Event

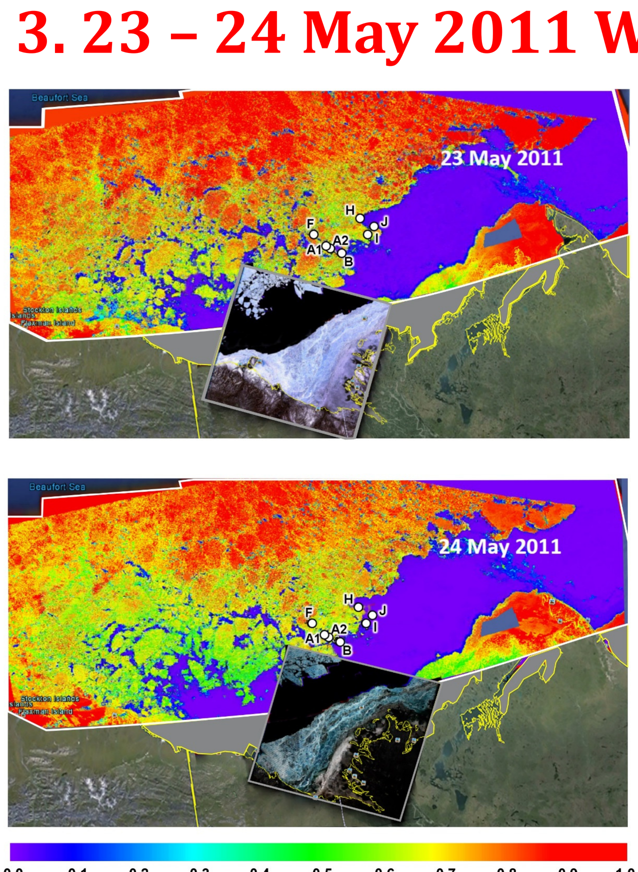

Figure 2. MODIS imagery showing surface albedo (surface brightness return) and with available LANDSAT imagery overlain for 23 May 2011 (top) and 24 May 2011 (bottom).

Ice cover in the southern Beaufort Sea was typical for late May, with 9/10+ coverage of thick first-year sea ice (>120 cm) (Figure 1). Floe sizes at the ice edge over our study site (70.5°N 137.0°W to 71.3°N 134.0°W) ranged between 10 – 500 m for 23 – 24 May, 2011 (Figure 2). A large area of fetch emerged between 17 – 23 May 2011, where mobile pack ice was forced by strong winds westward away from the Canadian Archipelago and coastline (Figure 1). Wind forcing was predominantly easterly over the region from 13 – 21 May 2011 with average wind speeds of 12 - 15 m • s^{-1}. Winds then backed to southeasterlies (12 - 20 m • s^{-1}) on 22 May 2011, with the strongest winds (~20 m • s^{-1}) centred over the open water immediately north of Cape Bathurst. Fetch of 150 – 350 km for easterly winds in the Southern Beaufort Sea and Amundsen Gulf is centred at 71°N and extends east-west along 71°N from 123°W – 134°W (Figure 1). The ice edge is defined by the point where the IPS range data indicative of ice drafts (FY ice floes and keels) sharply switch to data indicative of open water and waves, with a commensurate drop in ice concentration to <1/10 ice cover (Figure 2).

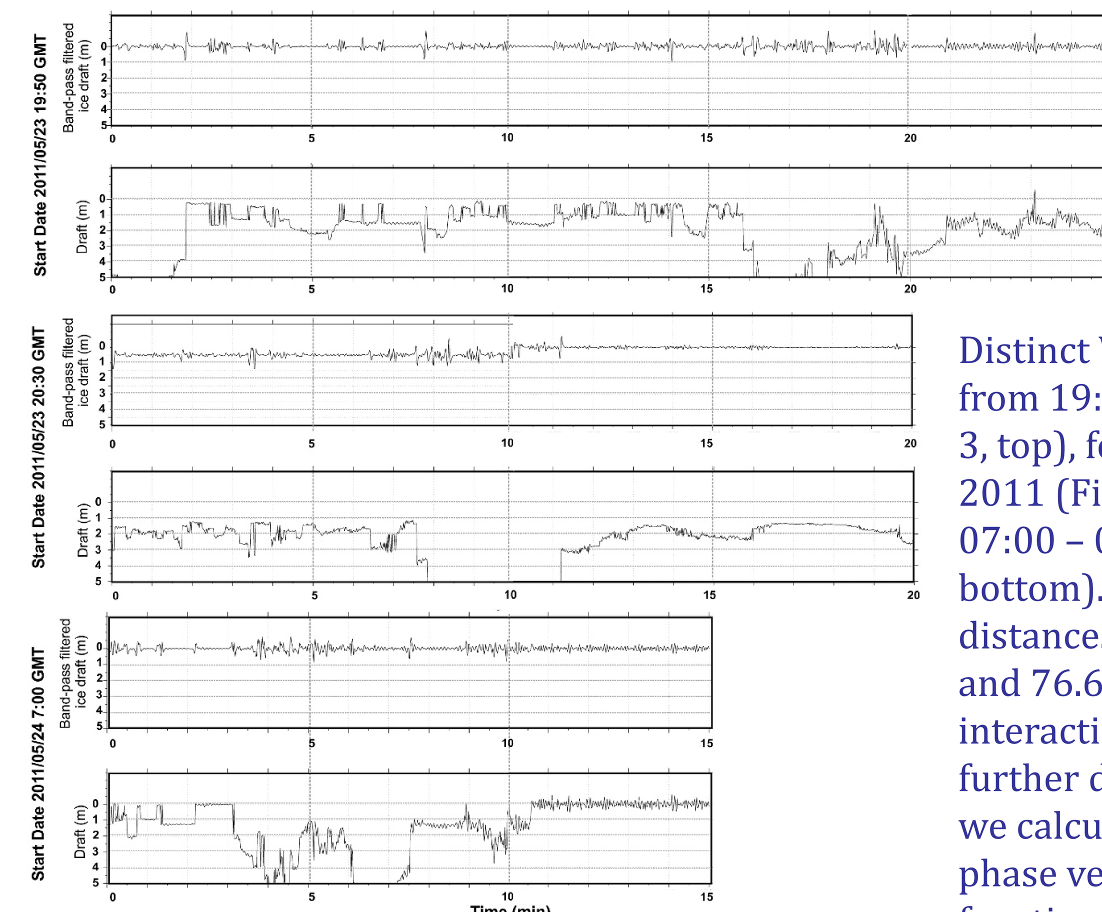

Figure 3: Top) Site H: first-order Butterworth bandpass filtered ice drafts (top) and original ice drafts (m) (bottom) 19:50 – 20:15 UTC, 23 – May 2011. Middle) Site B: first-order Butterworth bandpass filtered ice drafts (top) and original ice drafts (m) (bottom) 20:40 – 20:50 UTC, 23 – May 2011. Bottom) Site I: first-order Butterworth bandpass filtered ice drafts (top) and original ice drafts (m) (bottom) 07:00 – 07:15 UTC, 23 – May 2011. (0.1 – 0.33Hz cutoff frequencies) .

Distinct WII events were identified at site H from 19:50 – 20:15 UTC 23 May 2011 (Figure 3, top), for Site B from 2040 – 2050 May 23 2011 (Figure 3, middle), and for Site I from 07:00 – 07:15 24 May 2011 (Figure 3, bottom). Wave penetration was detected at distances from the ice edge (D) of 142.6 m and 76.6 m at site H and I, respectively. The interaction of waves with the ice cover is further divided into time segments, for each we calculate period (T), wavelength (l), wave phase velocity (v_p), and wave height as a function of D ((H (D)).

T = 5.0 s, l = 37.5 and v_p = 3.3 m • s^{-1} were determined for both sites. Average ice velocities during the WII events were 13.2 cm • s^{-1} towards the west at both sites. Site B (Figure 3, middle) permits us to identify the arrivals of waves propagating through the pack ice from Site H ~25 minutes later. High ice draft variability during these arrivals ruled out meaningful determination of H(D) values.

4. Reflection and Attenuation of Waves

Information regarding the attenuation of waves was extracted for sites H and I during the WII event (Table 1 & 2). Attenuation coefficients are estimated for a WII event on 23 – 24 May 2011 for sites H and site I by non-linear least-squares fit (Figure 4) using equation 1.

Table 1. Site H

Time (HH:MM:SS)UTC	Description	D (m)	Floe Size (m)	Mean Ice Draft (m)	H(m)
20:15:00	o/w	n/a	n/a	n/a	1.02*
20:13:08	irregular	0-14.8	14.8	1.5	0.7
20:13:06	o/w	14.8-15.0	0.2	-	-
20:10:57	level floe	15.0-32.1	17.1	1.6	0.63
20:10:56	floe boundary	32.1-32.2	0.1	-	-
20:09:10	level keel	32.2-46.2	14.0	3.1	0.45
20:09:09	floe boundary	46.2-46.3	0.1	-	-
20:06:08	keel	46.3-70.2	23.9	4.9	0.24
20:06:07	boundary	70.2-70.4	0.2	-	-
20:05:53	irregular floe	70.4-72.2	1.8	3.3	0.21
20:05:52	floe boundary	72.2-72.3	0.1	-	-
20:05:44	level keel	72.3-73.4	1.1	1.0	n/a
20:05:43	o/w crack	73.4-73.5	0.1	-	-
20:05:01	small floe	73.5-79.1	5.6	0.7	n/a
20:05:00	o/w crack	79.1-79.2	0.1	-	-
20:04:09	small floe	79.2-85.9	6.7	1.6	n/a
20:04:08	o/w crack	85.9-86.1	0.2	-	-
20:03:13	small floe	86.1-93.3	7.2	0.8	n/a
20:03:12	o/w crack	93.3-93.5	0.2	-	-
20:02:43	small floe	93.5-97.3	3.8	1.0	n/a
20:02:42	o/w crack	97.3-97.4	0.1	-	-
20:02:41	level floe	97.4-109.3	11.9	0.8	n/a
20:01:11	o/w crack	109.3-109.4	0.1	-	-
19:59:52	level floe	109.4-119.9	10.5	1.6	0.19
19:59:51	o/w crack	119.9-120.0	0.1	-	-
19:58:25	irregular floe	120-131.3	11.3	0.8	n/a
19:58:24	o/w crack	131.3-131.5	0.2	-	-
19:57:50	small floe	131.5-136.0	4.5	2.0	n/a
19:57:49	o/w crack	136.0-136.1	0.1	-	-
19:56:47	level floe	136.1-144.3	8.2	1.6	0.15
19:56:39	o/w lead	144.3-145.3	1.0	-	-
19:56:17	small floe	145.3-148.2	2.9	1.5	n/a
19:56:15	floe boundary	148.2-148.5	0.3	-	-
19:55:42	level floe	148.5-152.5	4.0	1.3	0.12
19:55:41	o/w crack	152.5-153.0	0.5	-	-
19:54:11	level floe	153.0-164.9	11.9	1.9	n/a
19:54:02	o/w lead	164.9-166.1	1.2	-	-
19:53:51	small floe	166.1-167.5	1.4	1.5	n/a
19:53:28	o/w lead	167.5-170.5	3.0	-	-
19:52:59	small floe	170.5-174.4	3.9	1.2	n/a
19:52:42	o/w lead	174.4-176.6	2.2	-	-
19:52:41	small floe	176.6-176.7	0.1	1.5	n/a
19:51:53	o/w lead	176.7-183.1	6.4	-	-
19:50:00	deep keel	183.1-198.0	14.9	5.6	n/a

Table 2. Site I

Time (HH:MM:SS)UTC	Description	D (m)	Floe Size (m)	Mean Ice Draft (m)	H(m)
7:10:36	o/w	n/a	n/a	n/a	1.02*
7:10:04	irregular floe	0-4.2	4.2	1.3	0.71
7:09:58	o/w crack	4.2-5.02	0.8	-	-
7:08:57	irregular floe	5.0-13.1	8.1	1.8	0.55
7:08:56	o/w crack	13.1-13.2	0.1	-	-
7:07:40	level floe	13.2-23.4	10.2	1.3	0.52
7:07:39	o/w crack	23.4-23.5	0.1	-	-
7:06:01	5 - 8m keel	23.5 - 36.3	12.8	5.0	0.35
7:06:00	o/w crack	36.4 - 36.5	0.1	-	-
7:03:11	irregular floe	36.5 - 58.7	22.2	3.0	n/a
7:02:13	lead	58.7 - 66.4	7.6	-	-
7:01:21	level floe	66.4 - 73.3	6.86	1.2	0.11
7:01:15	o/w crack	73.3 - 74.1	0.8	-	-
7:00:51	level floe	74.1 - 77.2	3.1	1.0	0.1
7:00:46	o/w crack	77.2 - 77.9	0.7	-	-
7:00:28	level floe	77.9 - 80.3	2.4	1.8	n/a
7:00:27	o/w crack	80.3 - 80.4	0.1	-	-
7:00:00	irregular floe	80.4 - 83.8	3.4	0.8	n/a

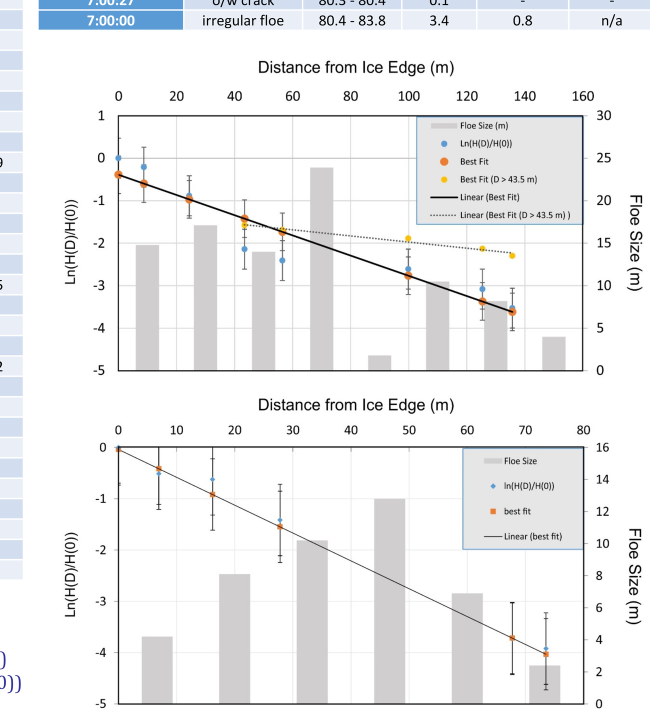

Figure 4. Attenuation coefficient analysis for site H (top) and site I (bottom) with respect to distance from the ice edge. Attenuation coefficients of α = 2.4 • 10^{-2} m^{-1} (site H) and α = 5.4 • 10^{-2} m^{-1} (site I) are determined by fitting a 'line of best fit' to values of Ln(H(D)/H(0)) calculated for site H (top), and site I (bottom).

The interaction of waves (T_P = 5.0 s and l ~37.5 m) with the ice pack reduced their amplitudes by wave reflection at the ice edge, and by scattering within the pack ice. We estimated reflection coefficients of 53% and 52% for Site H and Site I respectively. The estimated reflection coefficients are lower than expected for T_P = 5 s (Meylan & Squire, 1994) and this is likely due to the small floe size used for coefficient calculation at each site. This suggests that the initial 4.2 m floe at site I was equally effective at reflecting wave energy at T = 5.0 as the 14.8 m floe at site H.

Ice concentration and floe differences between the two sites may have affected wave reflection. Attenuation coefficients were calculated for sites H (α = 2.4 • 10^{-2} m^{-1}) and I (α = 5.4 • 10^{-2} m^{-1}) respectively. The larger α estimated for site I likely represents increased scattering and dissipation due to smaller floes and looser ice cover present in that case (ice concentration of ~9/10th as compared to 9/10th+ at site H). Thick keels are present in both cases, and had a clear impact on attenuation of waves within the ice pack evidenced by a smaller attenuation coefficient (a = 1.3 • 10^{-2} m^{-1}) for D > 43.5 m at site H. This effect may also be attributable to the underestimation of H_S(D) in ice floes > 10 m diameter, particularly if they were not centred on our linear sample transect or if ice conditions and drift velocities are not consistent over the 10-minute periods associated with our estimates.

5. Conclusions

Our estimated attenuation coefficients for short waves (< 6 s) appear to be greater than the values on the order of 10^{-5} – 10^{-3} m^{-1} reported in earlier studies (Meylan et al., 2014; Sutherland & Rabault, 2016). Wadhams et al., (1986) presented attenuation data obtained in a field of small Antarctic pack ice floes 0.5 – 2.0 km from the ice edge corresponding to α = 4.5 • 10^{-4} m^{-1} for T = *6 s.* Meylan et al., (2014) showed attenuation coefficients of order 10^{-3} m^{-1} follow a non-linear fit to the inverse fourth power of wave period for short waves, implying rapid attenuation occurs at T_P < 10 s. Liu et al., (1991) observed an attenuation rate of 1.6 • 10^{-3} m^{-1} at T = 7.5 s in ice floes < 20 m in diameter and about 1.5 m thick. Attenuation rates estimated in our case are high as compared with earlier field estimates, and likely suggest there is no rollover effect, in agreement with Wadhams et al., (1988).

Key References

Marko, J.R., 2003. Observations and analyses of an intense waves-in-ice event in the Sea of Okhotsk, J. Geophys. Res. ***108****(C9), 3296, doi: 10.1029/2001JC001214.*

Meylan, M., L. G. Bennetts, and A. L. Kohout, 2014. In situ measurements and analysis of ocean waves in the Antarctic marginal ice zone, Geophys. Res. Lett., ***41****, 5046–5051, doi:10.1002/2014GL060809.*

Wadhams, P., Squire, V.A., Goodman, D.J., Cowan, A.M., and Moore, S.C., 1988. The attenuation of ocear waves in the marginal ice zone, J. Geophys. Res., ***93****, 6799– 6818, doi:10.1029/JC093iC06p06799.*

Data sources and Acknowledgments

NSERC-IRDF to Dr. Matthew Asplin
ArcticNet-Industry Partnership Program
Captains and Crew of the CCGS Amundsen
R. Bowen, D. Sadowy & D. Billenness

Contact

Dr. Matthew G. Asplin
Department of Geography
B-124 David Turpin Building
University of Victoria
British Columbia, Canada
Asplin@gmail.com
1-250-812-5446